Cancer Cell International

RESEARCH

Open Access

Exosome-mediated transfer of lncRNA RP3-340B19.3 promotes the progression of breast cancer by sponging miR-4510/MORC4 axis

Bo Wang[1†], Jiahui Mao[2†], Linxia Wang[3], Yuexin Zhao[3], Bingying Wang[3*] and Huan Yang[3*]

Abstract

Background This study aims to explore the molecular mechanism of lncRNA RP3-340B19.3 on breast cancer cell proliferation and metastasis and clinical significance of lncRNA RP3-340B19.3 for breast cancer.

Methods The subcellular localization of lncRNA RP3-340B19.3 was identified using RNA fluorescence in situ hybridization (FISH). The expression of lncRNA RP3-340B19.3 in breast cancer cells, breast cancer tissues, as well as the serum and serum exosomes of breast cancer patients, was measured through quantitative RT-PCR. In the in vitro setting, we conducted experiments to observe the effects of RP3-340B19.3 on both cell migration and proliferation. This was achieved through the utilization of transwell migration assays as well as clone formation assays. Meanwhile, transwell migration assays and clone formation assays were used to observe the effects of MDA-MB-231-exosomes enriched in RP3-340B19.3 on breast cancer microenvironment cells MCF7 and BMMSCs. Additionally, western blotting techniques were used to assess the expression levels of proteins associated with essential cellular processes such as proliferation, apoptosis, and metastasis. In vivo, the impact of RP3-340B19.3 knockdown on tumour weight and volume was observed within a nude mice model. We aimed to delve into the intricate molecular mechanisms involving RP3-340B19.3 by using bioinformatics analysis, dual luciferase reporter gene experiments and western blotting. Moreover, the potential correlations between RP3-340B19.3 expression and various clinical pathological characteristics were analyzed.

Results Our investigation revealed that RP3-340B19.3 was expressed in both the cytoplasm and nucleus, with a noteworthy increase in breast cancer cells. Notably, we found that RP3-340B19.3 exerted a promoting influence on the proliferation and migration of breast cancer cells, both in vitro and in vivo. MDA-MB-231-exosomes enriched in RP3-340B19.3 promoted the proliferation and migration of MCF7 and BMMSCs in vitro. Mechanistically, RP3-340B19.3 demonstrated the capability to modulate the expression of MORC4 by forming a complex with miR-4510. This interaction subsequently triggered the activation of the NF-κB and Wnt-β-catenin signaling pathways. Furthermore, our study highlighted the potential diagnostic utility of RP3-340B19.3. We discovered its presence in the serum and

[†]Bo Wang and Jiahui Mao contributed equally to this work.

*Correspondence:
Bingying Wang
wangbingying416315@163.com
Huan Yang
zjyhcherry@126.com

Full list of author information is available at the end of the article

exosomes of breast cancer patients, showing promising efficacy as a diagnostic marker. Notably, the diagnostic potential of RP3-340B19.3 was particularly significant in relation to distinguishing between different pathological types of breast cancer and correlating with tumour diameter.

Conclusion Our findings establish that RP3-340B19.3 plays a pivotal role in driving the proliferation and metastasis of breast cancer. Additionally, exosomes enriched in RP3-340B19.3 could influence MCF7 and BMMSCs in tumour microenvironment, promoting the progression of breast cancer. This discovery positions RP3-340B19.3 as a prospective novel candidate for a tumour marker, offering substantial potential in the realms of breast cancer diagnosis and treatment strategies.

Keywords lncRNA RP3-340B19.3, Breast cancer, Proliferation, Metastasis, Exosome

Background

Breast cancer has emerged as the most prevalent malignancy afflicting women worldwide, claiming the highest incidence rate and ranking as the second leading cause of mortality [1]. The paramount strategy for addressing breast cancer lies in its early detection and precise therapeutic interventions, both of which are depend upon an intricate comprehension of the underlying pathogenesis [2]. The etiological framework of breast cancer is intricate, encompassing factors such as endocrine hormones, diverse genetic components, and epigenetic alterations [3]. Given this complexity, the pursuit of novel molecular markers and therapeutic targets assumes paramount significance. These endeavors hold the potential to extend the survival duration and enhance the quality of life for individuals grappling with breast cancer.

Long noncoding RNA (lncRNA) represents a class of noncoding RNA molecules characterized by their length, exceeding 200 nucleotides [4, 5]. These transcripts exhibit expression within specific tumour cell types or tissues, exerting significant functional roles [6]. A notable feature of lncRNAs is their pronounced tissue specificity and spatiotemporal expression patterns. Involved in a diverse range of cellular processes, lncRNAs influence functions such as cell cycle regulation, apoptosis modulation, and maintenance of genomic stability [7]. Mounting research endeavors underscore the pivotal role of lncRNAs in various facets of tumorigenesis. These encompass the initiation, progression, metastasis, and even resistance to therapeutic interventions in cancer [8–11]. For instance, the lncRNA-BC069792 exhibits the potential to function as a competing endogenous RNA (ceRNA), sequestering miR-658 or miR-4739. This interaction consequently augments the expression of the downstream target gene KCNQ4. Concurrently, it impedes the activity of JAK2 and p-AKT, thereby slowing the progression of breast cancer [12]. Likewise, the lncRNA HOTAIR modulates the miR-20a-5p/HMGA2 axis, promoting breast cancer cell proliferation and metastasis while suppressing apoptosis [13]. Furthermore, the lncRNA MALAT1 assumes a role in fostering breast cancer advancement and exacerbating doxorubicin resistance. This effect is mediated through its interaction with miR-570-3p [14]. Collectively, these findings underscore the crucial contribution of lncRNAs to the pathogenesis of breast cancer. Consequently, they emerge as potential novel biomarkers for both the diagnosis and treatment of this condition.

Exosomes are membranous vesicles measuring 40–100 nm in diameter. They are released into the extracellular space when multivesicular bodies fuse with the plasma membrane [15]. Exosomes play important roles in intercellular communication, and can transfer proteins, mRNAs, and noncoding RNAs to recipient cells by fusing with target cell membranes [16]. They can also transfer cellular contents from tumour cells to tumour microenvironmental cells, thereby promoting tumour progression. The lncRNAs loaded into exosomes are transferred to nearby cells or target cells at a distant location, where they regulate signaling pathways related to cell proliferation, differentiation, and apoptosis [17]. Ni et al. found that breast cancer-derived exosomes could transmit lncRNA SNHG16 to induce CD73+γδ1 Treg cells [18]. Exosomal lncRNA Linc00969 could induce trastuzumab resistance by increasing HER-2 protein expression and mRNA stability by binding to HUR [19].

Previous research conducted by our team has strongly implicated Toll-like receptor 4 (TLR4) activation in breast cancer metastasis. Specifically, the activation of TLR4 through bacterial lipopolysaccharide (LPS) has been demonstrated to trigger the TLR4/MyD88/NF-κB signaling pathway, thereby facilitating the metastasis of breast cancer cell lines both in vivo and in vitro [20]. In our pursuit of understanding the potential involvement of lncRNAs in this process, we employed chip screening technology. Notably, our screening efforts unveiled a significant upregulation of the LncRNA RP3-340B19.3 in breast cancer cells upon TLR4 activation. Remarkably, there exists a notable gap in the existing literature concerning the expression and functional analysis of RP3-340B19.3. This article addresses this gap by demonstrating that RP3-340B19.3 exhibits heightened expression levels within breast cancer tissues. Additionally, it exerts regulatory control over MORC family CW type zinc finger 4 (MORC4) expression, consequently leading

to the activation of both NF-κB and Wnt-β-catenin signaling pathways. Importantly, this regulatory effect is mediated by RP3-340B19.3's direct interaction with miR-4510 within the context of breast cancer. Furthermore, the potential clinical significance of RP3-340B19.3 is underscored. Its presence in both serum and serum exosomes from breast cancer patients points toward its potential utility as a non-invasive tumour marker for breast cancer diagnosis. In summation, this study sheds light on the unexplored territory of RP3-340B19.3, revealing its pivotal role in breast cancer by regulating crucial signaling pathways and suggesting its promise as a diagnostic marker.

Materials and methods

Clinical specimens

Blood samples were procured from female patients diagnosed with breast cancer, and their age-matched healthy counterparts served as the control group. Notably, the patients had not undergone any form of treatment prior to their surgical procedures. Subsequent to centrifugation at 4 °C and 3000 rpm for 15 min, the resulting blood components were meticulously transferred into new EP tubes. Further centrifugation at 4 °C and 12,000 g for 10 min facilitated the separation of additional cellular materials. The isolated serum was then securely stored within a -80 °C refrigerator for prospective use. Moreover, female patients afflicted with primary breast cancer were selected for tissue collection. Paired adjacent paracancerous tissues, situated at a distance of more than 5 cm from the primary lesion, were also gathered. Rigorous scrutiny by two pathologists confirmed the authenticity of all specimens. The categorization of these samples adhered to the histological grading criteria outlined by the World Health Organization (WHO). The collection of all specimens was undertaken with explicit consent from both patients and healthy controls, and the protocol was granted approval by the hospital's ethics committee (Project Number: JD-LK-2019-065-01).

Cell Culture

The human breast cancer cell lines, MCF-7 and MDA-MB-231, 293T and BMMSCs were obtained from the cell bank of the Chinese Academy of Sciences. MCF-7, MDA-MB-231 and 293T cell lines were cultivated in a medium supplemented with 10% fetal bovine serum (Gibco, Grand Island, NY), while the BMMSCs cell line was cultivated in a medium supplemented with 15% fetal bovine serum. Incubation was carried out in a 37 °C environment with 5% CO_2.

Microarray analysis

Total RNA was isolated from control MDA-MB-231 cells and LPS-stimulated MDA-MB-231 using TRIzol reagent (Invitrogen) as described by the manufacturer's protocol. The lncRNA microarray was performed by Affymetrix Human Transcriptome Array 2.0 (HTA 2.0) GeneChips (Affymetrix, Santa Clara, CA, USA) The differentially expressed lncRNAs were analyzed with the criteria of $P<0.05$ and fold-change > 2.0.

Cell transfection

A density of 1×10^5 breast cancer cells per well was introduced into each well of a 6-well plate. Following an overnight period to ensure attachment, transfection procedures were initiated. The RP3-340B19.3 eukaryotic vector and RP3-340B19.3 siRNA fragment were separately reconstituted in serum-free culture medium, each with a total volume of 250 µl. For comparison, the pcDNA empty vector and NC (negative control) were employed as the control groups. The process of cell transfection was executed using Lipofectamine 3000 (Invitrogen, Carlsbad, CA, USA). MiR-4510 mimics were introduced at a concentration of 100 nM, while miR-4510 inhibitor was added at 250 nM. Detailed sequences and modifications of the oligonucleotides used in these experiments can be found in Supplementary Table S1.

RNA extraction and RT-PCR

Utilize various RNA extraction kits to extract total RNA from breast cancer cells, tissues, serum, and serum exosomes (Invitrogen). Perform reverse transcription to obtain cDNA, and then store the product at -20 ℃ for future use (Vazyme, China). Prepare the quantitative PCR system, setting the conventional parameters with an annealing temperature of 55 ℃, and amplify for 45 cycles (Vazyme, China). Analyze the expression differences between each group using the relative quantification method known as the $2^{-\Delta\Delta Ct}$ method.

Western blot detection

Prepare a polyacrylamide gel with a concentration ranging from 10 to 12% for SDS-PAGE. Load each well with approximately 50% of the desired total protein mass in micrograms (µg). Execute the electrophoresis procedure with a voltage of 80 V for the stacking gel and 100 V for the separation gel. Upon completion of electrophoresis, transfer the separated proteins from the gel to a PVDF membrane utilizing an electrotransfer apparatus. Maintain a constant current of 350 mA for a duration of 2 h during the transfer process. Following the transfer, immerse the PVDF membrane in a solution of 5% skimmed milk at room temperature. Incubate the membrane on a shaking table for 1 h to block non-specific binding sites. Introduce primary antibodies against specific targets such as N-cadherin, E-cadherin, Vimentin, PCNA, Bcl2, GAPDH, etc., onto the membrane. Incubate the membrane overnight at a temperature of 4 ℃. On

the subsequent day, wash the membrane with 1x TBST buffer solution 3 times, allotting 10 min for each washing step. Subsequently, introduce a secondary antibody labeled with horseradish peroxidase (HRP) at a dilution of 1:1500. Incubate the membrane at a temperature of 37 ℃ for 1 h. Conduct 1x TBST buffer solution washes on the membrane, repeating the process 5 times, and allowing 10 min for each wash. Apply an enhanced chemiluminescence (ECL) solution to the membrane to initiate light emission. This should be done in a darkroom to enhance sensitivity. Once the ECL reaction is complete, wait for the membrane to dry before proceeding to the scanning step. The sources of antibodies were: E-cadherin, N-cadherin, p65, p-p65, slug, caspase3, PARP, β-catenin (Cell Signaling Technology, Beverly, MA, USA); vimentin, PCNA, Bcl2 (Bioworld Technology, Louis Park, MN, USA); twist (Abcam, Cambridge, MA); GAPDH, goat anti-rabbit IgG (HRP), and goat anti-mouse IgG (HRP) (Kangcheng, Shanghai, China).

Extraction of serum exosomes

Aspirate 250 μL of serum into an EP tube, then add 63 μL of serum exosome extraction reagent (System Biosciences, Mountain View, CA, USA). Place the mixture at 4℃ for at least 12 h. Afterward, remove the mixture from 4℃ and centrifuge it at 1500 g for 30 min, and then at 3000 g for 5 min. Discard the upper liquid each time. Next, add 50% of the solution, which has been sterilized under high pressure, to the EP tube, followed by 50 μL of PBS. Pipette the mixture repeatedly until it turns into a yellowish transparent clear liquid, and then set it aside for further use.

Analysis of luciferase reporter gene

The 3'-UTR mRNA of wild-type RP3-340B19.3 was obtained using the PCR method and then ligated to the pmirGLO double luciferase targeted expression vector (Promega, Madison, WI). Additionally, the 3'-UTR mutant structure of RP3-340B19.3 was constructed and connected to the double luciferase targeting vector. The reporter gene vector, miR-4510 mimics, and MNC were co-transfected into 293T cells. After 24 h, the fluorescence signal value was collected, and the intensity of fluorescence change was analyzed (Agilent Technologies, Santa Clara, CA).

RNA fluorescence in situ hybridization

After high-pressure sterilization of pre-prepared cell slides, they are placed in a cell culture plate. Cells are seeded at a certain density and cultured overnight in a cell culture incubator. The cell density on the second day reaches approximately 20-50%. Next, the cell supernatant is removed, and formalin is added to the culture plate for 30 min to fix the cells. The fixed solution is then discarded, and the plate is washed twice with PBS. After that, Buffer A is added to the culture plate at 100 μL and incubated for 15 min before being discarded. The plate is gently washed twice with PBS. Next, 100 μL of 2x Buffer C is added to the culture plate and incubated at 37℃ for 30 min. Meanwhile, the water bath pot is preheated to 73℃, and Buffer E is heated. The probe is diluted to a concentration of 100 μM with DEPC water. A probe mixture is prepared, which is then denatured at 73℃ for 5 min. The probe mixture is then dropped onto the cell slide and placed in a humid box at 37℃ overnight. The cell slides are removed and preheated, and 100 μL of Buffer F is dripped onto them, followed by a 5-minute wash. Another 100 μL of 2x Buffer C is dropped onto the cell slides and washed for an additional 5 min. DAPI is added dropwise to the cell culture plate to stain the nuclei, and incubated in the dark for 15 min. After washing with PBS twice, the coverslip is removed, sealed, and photos are taken for analysis (Agilent Technologies, Santa Clara, CA).

Plate clone formation and Transwell Experiment

1000 cells were inoculated into a small Petri dish, and the solution was changed routinely. Once a noticeable difference in trends was observed, the cells were fixed with formalin at room temperature for 15 min to halt growth. Subsequently, the cells were subjected to a 15-minute Crystal Violet staining, followed by a PBS wash and air-drying for photographic purposes.

For the lower chamber, 600 μL of serum-containing culture medium was added, while the cells were resuspended in serum-free culture medium. About 1×10^5 cells were then placed in the transwell chamber. Based on distinct treatment factors and cell growth characteristics, the upper chamber was removed after a designated period of cultivation. Initially, formalin was employed to fix the cells for 30 min. Later, cotton swabs were utilized to eliminate the cells adhering to the inner surface of the chamber membrane. A subsequent 20-minute Crystal Violet staining ensued, succeeded by thorough washing, gentle mounting, and natural drying. The number of cells that migrated to the outer surface beneath the membrane was subsequently quantified under both low-power and high-power microscopes.

Nude mouse breast subcutaneous transplantation Tumour Model

Twelve female BALB/c nude mice, aged 4–6 weeks, were utilized for this study. These mice were obtained from the Nanjing Model Animal Research Institute and were subsequently divided into two distinct groups. Each group received injections of either NC or RP3-340B19.3 siRNA transfected MDA-MB-231 cells, with a dose of 5×10^6 cells in 200 μL of PBS per mouse ($n=6$). Following cell

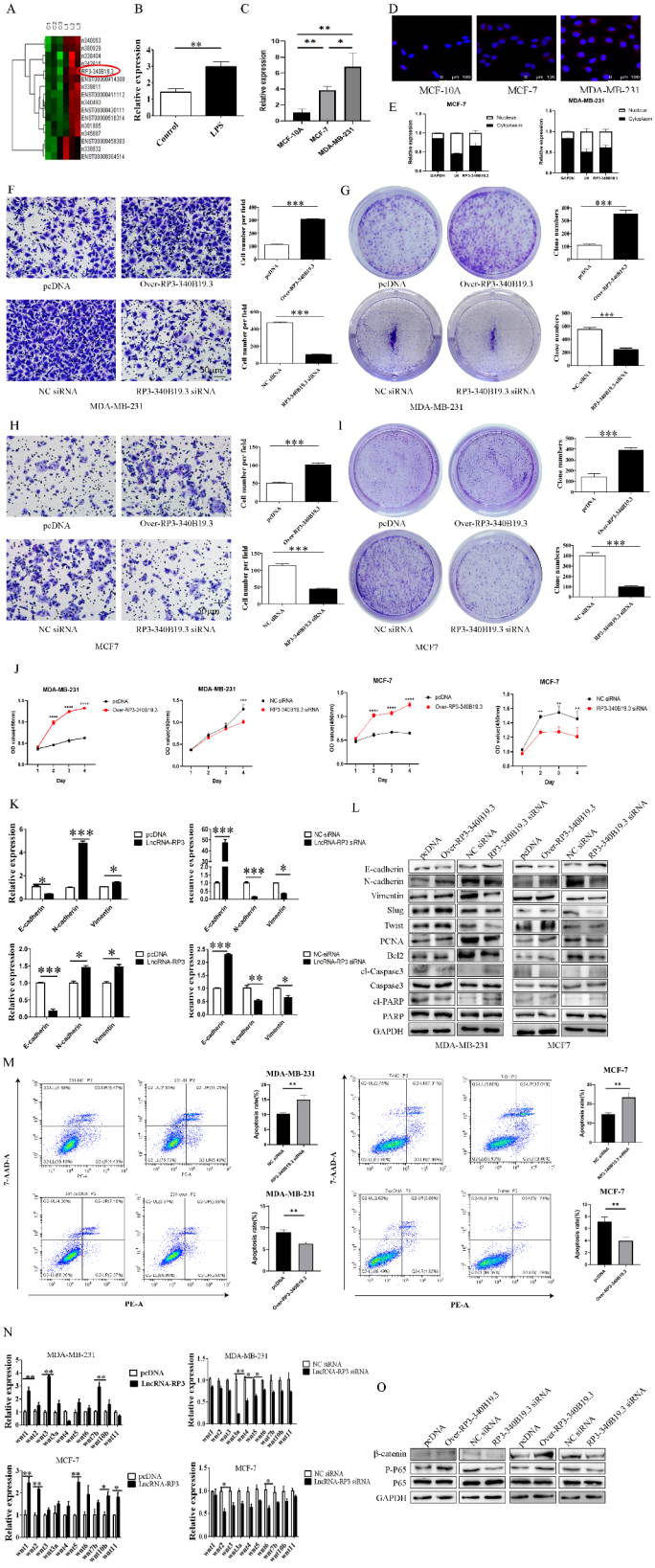

Fig. 1 (See legend on next page.)

(See figure on previous page.)

Fig. 1 RP3-340B19.3 promotes proliferation and migration of breast cancer in vitro. (**A**) Gene chip screening and bioinformatics prediction were used to select lnc RP3-340B19.3 as the subject of investigation. C, control MDA-MB-231; L, LPS treated MDA-MB-231. The concentration of LPS was 10 μg/ml. (**B**) The expression of RP3-340B19.3 in LPS-stimulated MDA-MB-231 breast cancer cells was examined by quantitative RT-PCR. The concentration of LPS was 10 μg/ml. $^{**}P < 0.01$. (**C**) The expression of RP3-340B19.3 in MDA-MB-231 and MCF7 was examined by quantitative RT-PCR. $^{*}P < 0.05$. (**D**) The expression of RP3-340B19.3 in MCF10A, MCF7 and MDA-MB-231 was examined by FISH. (**E**) To determine the cellular localization of RP3-340B19.3, the fractionation experiment was performed using digitonin. The level of GAPDH and U6 were checked for verification of cytoplasmic and nuclear extracts, respectively. The levels of RP3-340B19.3 mRNA were determined by RT-qPCR. (**F**) The migratory ability of RP3-340B19.3-overexpressing and RP3-340B19.3-knockdown MDA-MB-231 cells were evaluated by transwell migration assay. $^{***}P < 0.001$. (**G**) The proliferation ability of RP3-340B19.3-overexpressing and RP3-340B19.3-knockdown MDA-MB-231 cells were evaluated by cell colony assay. $^{***}P < 0.001$. (**H**) The migratory ability of RP3-340B19.3-overexpressing and RP3-340B19.3-knockdown MCF7 cells were evaluated by using transwell migration assay. $^{***}P < 0.001$. (**I**) The proliferation ability of RP3-340B19.3-overexpressing and RP3-340B19.3-knockdown MCF7 cells were evaluated by cell colony assay. $^{***}P < 0.001$. (**J**) The proliferation ability of RP3-340B19.3-overexpressing and RP3-340B19.3-knockdown MCF7 and MDA-MB-231 cells were evaluated by CCK8. $^{***}P < 0.001$, $^{**}P < 0.01$, $^{*}P < 0.05$. (**K**) The expression of EMT related genes in RP3-340B19.3-overexpressing and RP3-340B19.3-knockdown cells was examined by using quantitative RT-PCR. $^{***}P < 0.001$, $^{**}P < 0.01$, $^{*}P < 0.05$. (**L**) The expression of EMT related proteins, cleaved caspase3, PARP, PCNA and Bcl2 in RP3-340B19.3-overexpressing and RP3-340B19.3-knockdown cells was examined by using western blot. (**M**) The apoptosis rate of MCF7 cells pretreated with pcDNA, RP3-340B19.3 overexpression plasmids, NC siRNA, and RP3-340B19.3 siRNA. $^{**}P < 0.01$. (**N**) The expression of wnt-β-catenin related genes in RP3-340B19.3-overexpressing and RP3-340B19.3-knockdown cells was examined by using quantitative RT-PCR. $^{**}P < 0.01$, $^{*}P < 0.05$. (**O**) The expression of β-catenin, P-P65 in RP3-340B19.3-overexpressing and RP3-340B19.3-knockdown cells was examined by using western blot

injections, the tumorigenic timeline and tumour growth were meticulously monitored and recorded at two-day intervals. On approximately the 18th day, the nude mice were humanely euthanized. Tumours were then excised, weighed, subjected to paraffin sectioning, and stained using the HE staining method. Tumour volume was calculated using the formula: $V = (\text{length} \times \text{width}^2) / 2$.

Statistical analysis

Statistical analysis and graphical representation were carried out using SPSS and Prism software. The Wilcoxon signed rank test was applied to evaluate the expression level of RP3-340B19.3 in paired breast cancer and adjacent tissues. Additionally, a t-test was employed to assess the differences between the two groups. A significance threshold of $P<0.05$ was adopted to determine statistical significance.

Results

RP3-340B19.3 promotes proliferation and migration of breast cancer in vitro

Gene chip screening and bioinformatics prediction identified the long non-coding RNA (lncRNA) RP3-340B19.3 as the subject of investigation (Fig. 1A). Quantitative PCR confirmed a significant increase in the expression of lncRP3-340B19.3 in LPS-stimulated MDA-MB-231 breast cancer cells (Fig. 1B). Moreover, its expression in MDA-MB-231 was notably higher than that in MCF-7 cells (Fig. 1C). RNA Fluorescence in situ hybridization (FISH) analysis revealed the presence of RP3-340B19.3 in the cytoplasm and nucleus of MCF-10 A breast epithelial cells, MCF-7, and MDA-MB-231 breast cancer cell lines. Importantly, RP3-340B19.3 expression was significantly elevated in breast cancer cells (MDA-MB-231 and MCF7) compared to normal epithelial cells (MCF10A), suggesting its potential pro-cancer role (Fig. 1D). Meanwhile, to assess the localization of RP3-340B19.3, a cellular fractionation assay was conducted. The result revealed that RP3-340B19.3 were abundantly expressed in the cytosol (Fig. 1E). To further investigate its effects, MDA-MB-231 and MCF7 cells were transfected with pcDNA, RP3-340B19.3 overexpression plasmids, NC siRNA, and RP3-340B19.3 siRNA. Quantitative PCR results demonstrated increased RP3-340B19.3 expression in MDA-MB-231 and MCF7 cells following RP3-340B19.3 overexpression plasmid transfection, and decreased expression after RP3-340B19.3 siRNA transfection (Supplementary Fig. 1). Transwell migration assays indicated a significant increase in migratory cell numbers with RP3-340B19.3 overexpression and a reduction following RP3-340B19.3 siRNA transfection in MDA-MB-231 cells (Fig. 1F). Similarly, colony formation experiments indicated enhanced colony formation upon RP3-340B19.3 overexpression, and decreased cloning ability after RP3-340B19.3 knockdown (Fig. 1G). Comparable outcomes were observed in MCF7 cells, as RP3-340B19.3 overexpression bolstered migration and proliferation while knockdown reduced these capabilities (Fig. 1H and I). CCK8 results demonstrated that RP3-340B19.3 overexpression remarkably promoted the growth of MDA-MB-231 and MCF7 cells and RP3-340B19.3 knockdown inhibited the growth of MDA-MB-231 and MCF7 cells (Fig. 1J). Quantitative PCR analysis revealed that RP3-340B19.3 overexpression increased the expression of N-cadherin and Vimentin while suppressing E-cadherin. Conversely, RP3-340B19.3 knockdown led to decreased N-cadherin and Vimentin expression and increased E-cadherin expression (Fig. 1K). Western blot results demonstrated that RP3-340B19.3 overexpression downregulated E-cadherin expression and upregulated N-cadherin, Vimentin, Slug, and Twist expressions. Additionally, proliferation and apoptosis-related protein analysis displayed increased Bcl2 and PCNA expression, and decreased Caspase3 and

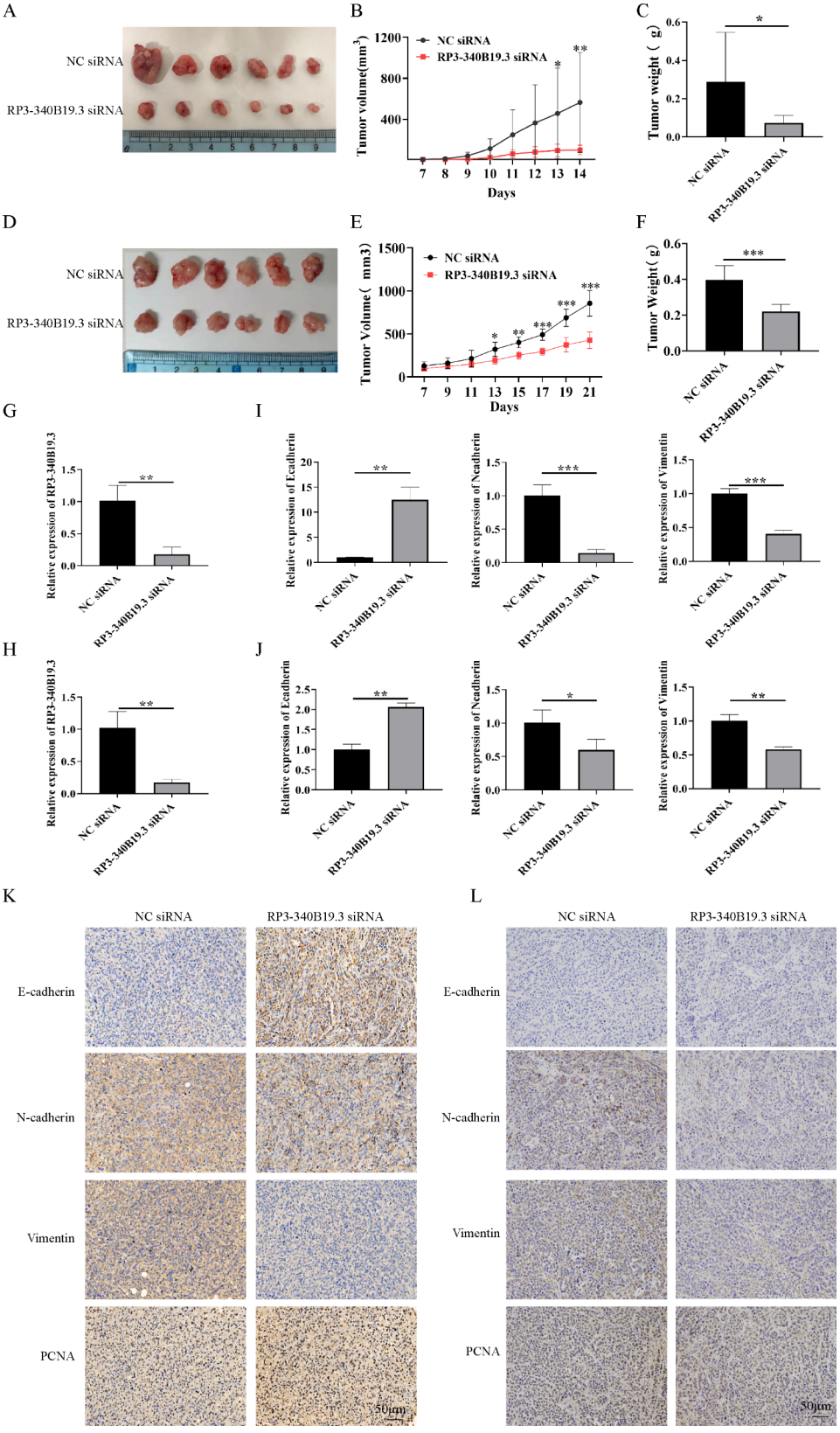

Fig. 2 (See legend on next page.)

(See figure on previous page.)

Fig. 2 RP3-340B19.3 promotes the proliferation and migration of breast cancer in vivo. (**A**), (**B**) and (**C**) The macroscopic appearance, volume and weight of subcutaneous tumours in mice($n=6$/group) transplanted with NC siRNA and RP3-340B19.3 siRNA transfected MDA-MB-231 cells. $^{**}P<0.01$, $^{*}P<0.05$. (**D**), (**E**) and (**F**) The macroscopic appearance, volume and weight of subcutaneous tumours in mice($n=6$/group) transplanted with NC siRNA and RP3-340B19.3 siRNA transfected MCF7 cells. $^{**}P<0.01$, $^{*}P<0.05$. (**G**) and (**H**) The expression of RP3-340B19.3 in the tumour tissues in mice transplanted with NC siRNA and RP3-340B19.3 siRNA transfected MDA-MB-231 and MCF7 cells was examined by using quantitative RT-PCR. $^{**}P<0.01$. (**I**) and (**J**) The expression of EMT related genes in mice with NC siRNA and RP3-340B19.3 siRNA transfected MDA-MB-231 and MCF7 cells was examined by using quantitative RT-PCR. $^{***}P<0.001$, $^{**}P<0.01$, $^{*}P<0.05$. (**K**) and (**L**) The expression of RP3-340B19.3 in the tumour tissues in mice transplanted with NC siRNA and RP3-340B19.3 siRNA transfected MDA-MB-231 cells was examined by using quantitative RT-PCR. $^{**}P<0.01$. (**H**) The expression of EMT related genes in mice with NC siRNA and RP3-340B19.3 siRNA transfected MDA-MB-231 cells was examined by using quantitative RT-PCR. $^{***}P<0.001$, $^{**}P<0.01$. (**K**) and (**L**) The expression of EMT related proteins and PCNA in mice transplanted with NC siRNA and RP3-340B19.3 siRNA transfected MDA-MB-231 and MCF7 cells was determined by using immunohistochemistry

PARP expression upon RP3-340B19.3 overexpression. Conversely, RP3-340B19.3 knockdown led to opposite changes in these proteins (Fig. 1L). The densitometric analysis of western blot results in Supplementary Fig. 4A. Meanwhile, we observed a significant decrease of apoptosis in RP3-340B19.3 overexpressing MDA-MB-231 and MCF7 cells compared to control cells. In contrary, RP3-340B19.3 knockdown could increase the apoptosis of MDA-MB-231 and MCF7 cells (Fig. 1M). To investigate the molecular mechanisms underlying the actions of RP3-340B19.3, related signaling pathway activation was explored. Quantitative PCR showed increased expression of several Wnt family genes (Wnt1, Wnt2, Wnt3, Wnt5, Wnt7b, Wnt10b, Wnt11) upon RP3-340B19.3 overexpression and decreased expression of Wnt2, Wnt3a, Wnt4, Wnt5, and Wnt6 after RP3-340B19.3 knockdown (Fig. 1N). Western blot analysis revealed elevated β-catenin expression in the RP3-340B19.3 overexpression group and reduced expression in the RP3-340B19.3 knockdown group. Additionally, RP3-340B19.3 overexpression led to increased phosphorylation of p65, while knockdown resulted in decreased phosphorylation of p65 (Fig. 1O). The densitometric analysis of western blot results in Supplementary Fig. 4B. Collectively, these findings suggest that lncRP3-340B19.3 promotes the proliferation and migration of breast cancer cells in vitro.

RP3-340B19.3 promotes the proliferation and migration of breast cancer in vivo

To gain deeper insights into the impact of RP3-340B19.3 on breast cancer proliferation and migration in vivo, we established subcutaneous tumour-bearing mouse models using RP3-340B19.3 knockdown MDA-MB-231 and MCF7 breast cancer cells. The outcomes revealed that the volume and weight of subcutaneous tumours in the RP3-340B19.3 siRNA transfection group were notably smaller than those in the NC siRNA transfection group. The difference in subcutaneous tumour volume continued to grow over time (Fig. 2A and F). Additionally, we assessed RP3-340B19.3 expression in subcutaneous tumour tissue. Compared to the control group, the RP3-340B19.3 siRNA transfection group exhibited lower expression levels (Fig. 2G and H). Quantitative PCR and immunohistochemistry analyses displayed elevated E-cadherin expression and decreased N-cadherin, Vimentin, and PCNA expression in the tumour tissue of the RP3-340B19.3 siRNA transfection group compared to the control group (Fig. 2I and L). Collectively, these findings underscore the role of RP3-340B19.3 in promoting breast cancer proliferation and metastasis within an in vivo context.

Role of RP3-340B19.3 in exosomes in tumour microenvironment

RP3-340B19.3 was significantly increased in MDA-MB-231-exosome compared with MCF10A-exosome and MCF7-exosome (Fig. 3A). To validate the role of RP3-340B19.3 delivered by exosomes from highly metastatic breast cancer cells in promoting breast cancer development, we conducted a series of experiments. First, we transfected MDA-MB-231 cells with pcDNA and RP3-340B19.3 overexpression plasmids, as well as with NC siRNA and RP3-340B19.3 siRNA. We collected the culture supernatant from these cells and isolated exosomes. These exosomes were then used to treat MCF7 cells, a low metastatic breast cancer cell line. Quantitative PCR results indicated that RP3-340B19.3 expression in MCF7 cells treated with Over-RP3-340B19.3-exosomes was higher compared to the pcDNA exosome group. Conversely, RP3-340B19.3 expression decreased in MCF7 cells treated with RP3-340B19.3 siRNA exosomes (Fig. 3B). Transwell migration and colony formation experiments demonstrated enhanced migration and colony formation ability in MCF7 cells after treatment with Over-RP3-340B19.3-exosomes (Supplementary Fig. 2). In contrast, MCF7 cells treated with RP3-340B19.3 siRNA exosomes exhibited reduced migration and colony formation ability (Fig. 3C and D). Quantitative PCR revealed decreased E-cadherin expression and increased N-cadherin and Vimentin expression in the Over-RP3-340B19.3 exosome treated group. The RP3-340B19.3 siRNA exosome treated group displayed the opposite trend (Fig. 3E). Western blot results showed downregulated E-cadherin expression and upregulated N-cadherin, Vimentin, Bcl2, and PCNA expressions in MCF7 cells treated with Over-RP3-340B19.3 exosomes. Conversely,

MCF7 cells treated with RP3-340B19.3 siRNA exosomes exhibited upregulated E-cadherin expression and downregulated N-cadherin, Vimentin, Bcl2, and PCNA expressions (Fig. 3F). The densitometric analysis of western blot results in Supplementary Fig. 4C.These findings suggest that exosomes derived from the highly metastatic MDA-MB-231 cells have the capability to transfer RP3-340B19.3 to the less metastatic MCF7 cells. This transfer ultimately leads to an enhancement in both proliferation and migration of the recipient cells, thereby contributing to the progression of breast cancer. Further investigation revealed that cancer-associated fibroblasts (CAFs), originating from bone marrow-derived mesenchymal stem cells (BMMSCs), play a relevant role in tumour development. Treating BMMSCs with exosomes from MDA-MB-231 cells (pcDNA ex, Over-RP3-340B19.3 ex, NC siRNA ex, RP3-340B19.3 siRNA ex) led to changes in RP3-340B19.3 expression levels. Over-RP3-340B19.3 exosome treatment increased RP3-340B19.3 expression, while RP3-340B19.3 siRNA exosome treatment decreased it (Fig. 3G). Transwell migration assays revealed enhanced migration in BMMSCs treated with Over-RP3-340B19.3 exosomes and reduced migration in those treated with RP3-340B19.3 siRNA exosomes (Fig. 3H). Immunofluorescence staining for α-SMA indicated elevated expression in the Over-RP3-340B19.3 exosome group and decreased expression in the RP3-340B19.3 siRNA exosome group (Fig. 3I). Quantitative PCR and Western blot analyses demonstrated that Over-RP3-340B19.3 exosome treatment increased N-cadherin and Vimentin expression, while reducing E-cadherin expression in BMMSCs. Conversely, RP3-340B19.3 siRNA exosome treatment led to decreased N-cadherin and Vimentin expressions and increased E-cadherin expression in BMMSCs (Fig. 3J and K). The densitometric analysis of western blot results in Supplementary Fig. 4D. Additionally, Western blot analysis revealed that the expression of β-catenin and phosphorylation of p65 was increased in BMMSCs treated by Over-RP3-340B19.3 exosome and was decreased in BMMSCs treated by RP3-340B19.3 siRNA exosomes (Fig. 3K). These results highlighted that MDA-MB-231 cells can transfer RP3-340B19.3 to BMMSCs in the breast cancer microenvironment via exosomes, thereby promoting breast cancer development.

RP3-340B19.3 targets and inhibits miR-4510

Utilizing PicTar and TargetScan bioinformatics tools, a potential target gene for RP3-340B19.3, miR-4510, was identified (Fig. 4A). To validate this interaction, reporter gene vectors containing wild-type and mutant binding sites for RP3-340B19.3 mRNA 3'-UTR were constructed. These vectors were co-transfected with miR-4510 mimics into 293T cells, and fluorescence intensity changes were measured. The results indicated that miR-4510 mimics significantly inhibited luciferase activity of the wild-type reporter gene vector, while the mutant vector remained unchanged (Fig. 4B). Further exploring the role of miR-4510, MDA-MB-231 and MCF7 cells were transfected with NC mimics, miR-4510 mimics, NC inhibitor, and miR-4510 inhibitor. Quantitative PCR revealed significantly increased miR-4510 expression in the miR-4510 mimics transfected group and reduced expression in the miR-4510 inhibitor transfection group (Supplementary Fig. 3). Simultaneously, miR-4510 expression was detected and found to be downregulated in the RP3-340B19.3 overexpression group and upregulated in the RP3-340B19.3 siRNA transfection group (Fig. 4C and D). Subsequent Transwell migration and colony formation experiments demonstrated reduced migration and colony formation ability in MDA-MB-231 cells upon miR-4510 overexpression, while these capabilities were enhanced with miR-4510 knockdown (Fig. 4E and F). Similar observations were made in the MCF7 cell line (Fig. 4G and H). Quantitative PCR results exhibited elevated E-cadherin expression and decreased N-cadherin and Vimentin expression in MDA-MB-231 and MCF7 cells transfected with miR-4510 mimics. Conversely, miR-4510 inhibitor transfection led to decreased E-cadherin expression and increased N-cadherin and Vimentin expressions (Fig. 4I). Western blot analysis revealed that elevated miR-4510 expression led to decreased N-cadherin, Vimentin, PCNA, and Bcl2 expressions, while increasing E-cadherin expression. Reduced miR-4510 expression had the opposite effect, increasing N-cadherin, Vimentin, PCNA, and Bcl2 expressions while decreasing E-cadherin expression (Fig. 4J). The densitometric analysis of western blot results in Supplementary Fig. 4E. These results collectively suggest that RP3-340B19.3 can target and inhibit miR-4510 expression, thus promoting breast cancer proliferation and metastasis.

miR-4510 targets and inhibits MORC4

Utilizing PicTar and TargetScan bioinformatics tools, MORC4 was identified as a potential target gene for miR-4510 (Fig. 5A). To validate this interaction, reporter gene vectors containing wild-type and mutant binding sites for MORC4 mRNA 3'-UTR were constructed. These vectors were co-transfected with miR-4510 mimics into 293T cells, and fluorescence intensity changes were measured. The results indicated that miR-4510 mimics significantly inhibited luciferase activity of the wild-type reporter gene vector, while the mutant vector remained unchanged (Fig. 5B). Quantitative PCR and Western blot results showed that miR-4510 overexpression in breast cancer cells led to decreased MORC4 expression, while miR-4510 downregulation increased MORC4 expression in both MDA-MB-231 and MCF7 cells (Fig. 5C and

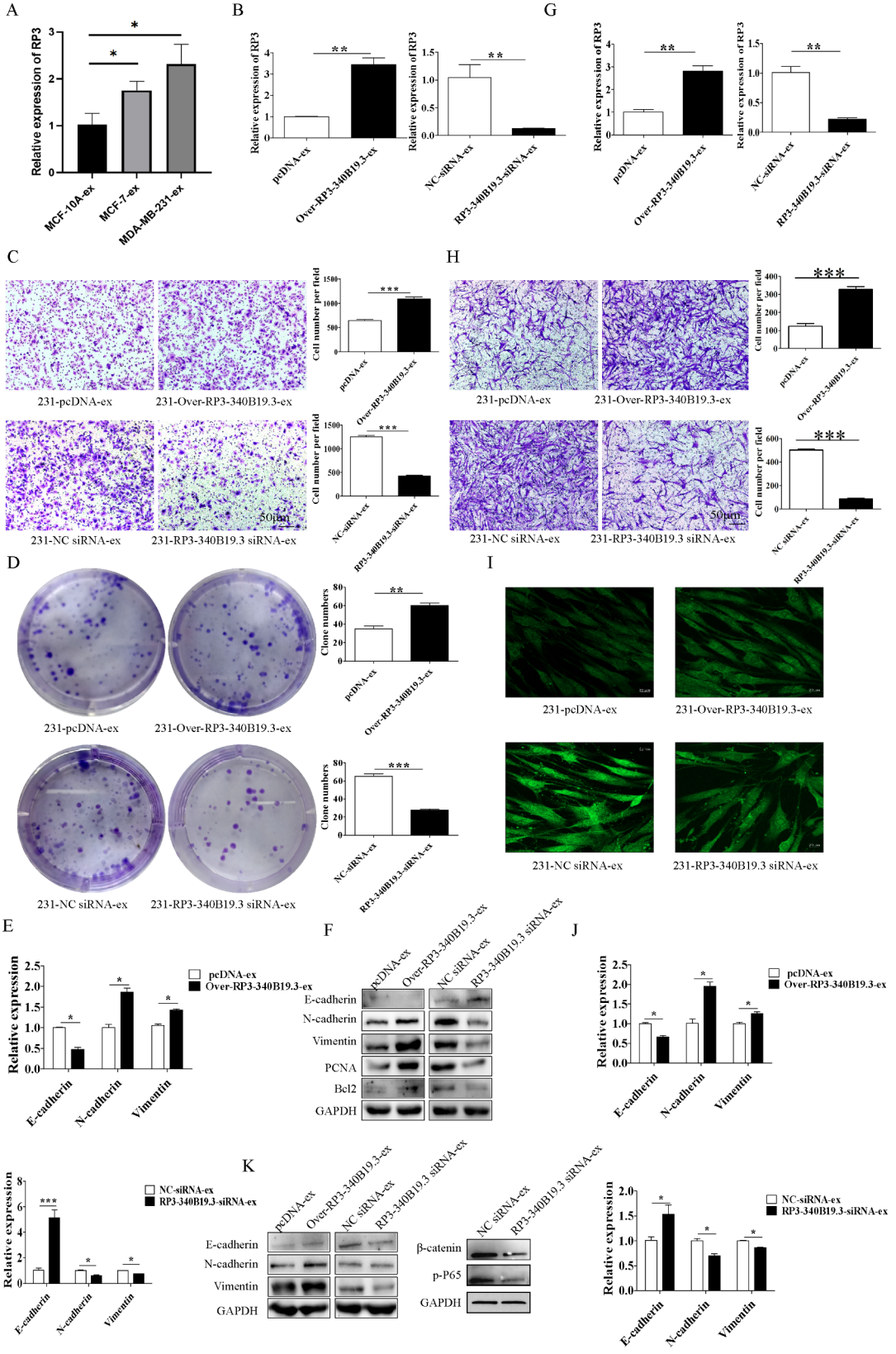

Fig. 3 (See legend on next page.)

(See figure on previous page.)

Fig. 3 Role of RP3-340B19.3 in exosomes in tumour microenvironment. (**A**) The expression of RP3-340B19.3 in MCF-10-ex, MCF7-ex and MDA-MB-231-ex was examined by using quantitative RT-PCR. *$P < 0.05$. (**B**) The expression of RP3-340B19.3 in MCF7 cells treated with 231-pcDNA-ex, 231-Over-RP3-340B19.3-ex, 231-NC-siRNA-ex and 231-RP3-340B19.3-siRNA-ex was examined by using quantitative RT-PCR. **$P < 0.01$. (**C**) The effect of 231-Over-RP3-340B19.3-ex and 231-RP3-340B19.3-siRNA-ex on the migration of MCF7. ***$P < 0.001$. (**D**) The effect of 231-Over-RP3-340B19.3-ex and 231-RP3-340B19.3-siRNA-ex on the proliferation of MCF7. ***$P < 0.001$, **$P < 0.01$. (**E**) The effect of 231-Over-RP3-340B19.3-ex and 231-RP3-340B19.3-siRNA-ex on the expression of EMT related genes in MCF7 was examined by using quantitative RT-PCR. *$P < 0.05$. (**F**) The effect of 231-Over-RP3-340B19.3-ex and 231-RP3-340B19.3-siRNA-ex on the expression of EMT related proteins, PCNA and Bcl2 in MCF7 was examined by using western blot. (**G**) The expression of RP3-340B19.3 in BMMSCs treated with 231-pcDNA-ex, 231-Over-RP3-340B19.3-ex, 231-NC-siRNA-ex and 231-RP3-340B19.3-siRNA-ex was examined by using quantitative RT-PCR. **$P < 0.01$. (**H**) The effect of 231-Over-RP3-340B19.3-ex and 231-RP3-340B19.3-siRNA-ex on the migration of BMMSCs. ***$P < 0.001$. (**I**) The expression of α-SMA in BMMSCs treated with 231-pcDNA-ex, 231-Over-RP3-340B19.3-ex, 231-NC-siRNA-ex and 231-RP3-340B19.3-siRNA-ex was examined by immunofluorescence. (**J**) and (**K**) The effect of 231-Over-RP3-340B19.3-ex and 231-RP3-340B19.3-siRNA-ex on the expression of EMT related genes in BMMSCs was examined by using quantitative RT-PCR and western blot. *$P < 0.05$. β-catenin and p-P65 was examined by using western blot

D). The densitometric analysis of western blot results in Supplementary Fig. 4F. In the animal model, immunohistochemistry results demonstrated increased MORC4 expression in the RP3-340B19.3 overexpression group and decreased MORC4 expression in the low expression group of RP3-340B19.3 (Fig. 5E). Quantitative PCR results indicated higher MORC4 expression in MDA-MB-231 compared to MCF10A and MCF7 cells (Fig. 5F). Furthermore, quantitative PCR and immunohistochemistry revealed elevated MORC4 expression in breast cancer tissue compared to normal breast tissue (Fig. 5G and H). To delve deeper into MORC4's function, NC siRNA and MORC4 siRNA were transfected into breast cancer cell lines MCF7 and MDA-MB-231, respectively. Quantitative PCR and Western blot results demonstrated significantly decreased MORC4 expression in the MORC4 siRNA transfected group compared to the control group (Fig. 5I and J). The densitometric analysis of western blot results in Supplementary Fig. 4G. WB results revealed that MORC4 could increase the expression of N-cadherin, and decrease the expression of E-cadherin (Fig. 5K). Transwell migration and colony formation experiments revealed reduced proliferation and migration abilities in breast cancer cells after MORC4 knockdown (Fig. 5L and M). Collectively, these results suggest that RP3-340B19.3 can promote breast cancer proliferation and metastasis by regulating MORC4 expression through its interaction with miR-4510.

Clinical detection analysis of RP3-340B19.3 in serum and its exosomes

To determine the expression level and significance of the RP3-340B19.3 in clinical samples, we conducted an investigation into its expression within the serum of breast cancer patients. Utilizing quantitative PCR analysis, we observed that the expression of lnc RP3-340B19.3 was significantly higher in 66 breast cancer patients compared to healthy controls (Fig. 6A). The results from the receiver operating characteristic (ROC) analysis exhibited a diagnostic sensitivity of 69.88% and a specificity of 75.64% for RP3-340B19.3 within the serum, with an area under the curve of 0.785 (Fig. 6B). When considering clinicopathological characteristics, we found a substantial increase in RP3-340B19.3 expression in the serum of breast cancer patients with tumour diameters greater than 2 cm and a pathological type of invasive ductal carcinoma. However, no significant relationship was observed with other pathological characteristics (Table 1). Previous studies have suggested that bioactive substances enriched in exosomes could serve as novel molecular markers for diagnosing breast cancer. In this context, we isolated exosomes from 27 pairs of both healthy controls and breast cancer patients to detect the expression of RP3-340B19.3. The outcomes indicated a significant elevation in RP3-340B19.3 expression within serum exosomes of breast cancer patients (Fig. 6C). ROC analysis demonstrated a diagnostic sensitivity of 83.87%, specificity of 70.37%, and an area under the curve of 0.794 for RP3-340B19.3 within serum exosomes (Fig. 6D). Notably, the analysis of clinicopathological characteristics revealed a significant correlation between RP3-340B19.3 expression in serum exosomes and tumour diameter, but no such correlation was observed with other pathological characteristics (Table 2). Furthermore, employing quantitative PCR, we assessed the expression of RP3-340B19.3 in 10 pairs of breast cancer tissues and adjacent tissues, revealing a markedly higher expression level in breast cancer tissues compared to adjacent tissues (Fig. 6E). Additionally, we evaluated the expression of miR-4510 in the serum of 35 pairs of healthy controls and breast cancer patients, finding a significantly lower level of miR-4510 in the serum of breast cancer patients relative to healthy controls (Fig. 6F). ROC analysis for miR-4510 exhibited a sensitivity of 73.33%, specificity of 66.67%, and an area under the curve of 0.756 for breast cancer diagnosis (Fig. 6G). Through clinical case data analysis, we identified a significant negative correlation between the expression level of miR-4510 and tumour diameter, as well as pathological type (Table 3). In conclusion, our findings suggest that RP3-340B19.3 within serum and serum exosomes has the potential to serve as a novel molecular marker for diagnosing breast cancer. Moreover, both RP3-340B19.3 and miR-4510 in the serum show promise as potential combined diagnostic indicators for breast cancer.

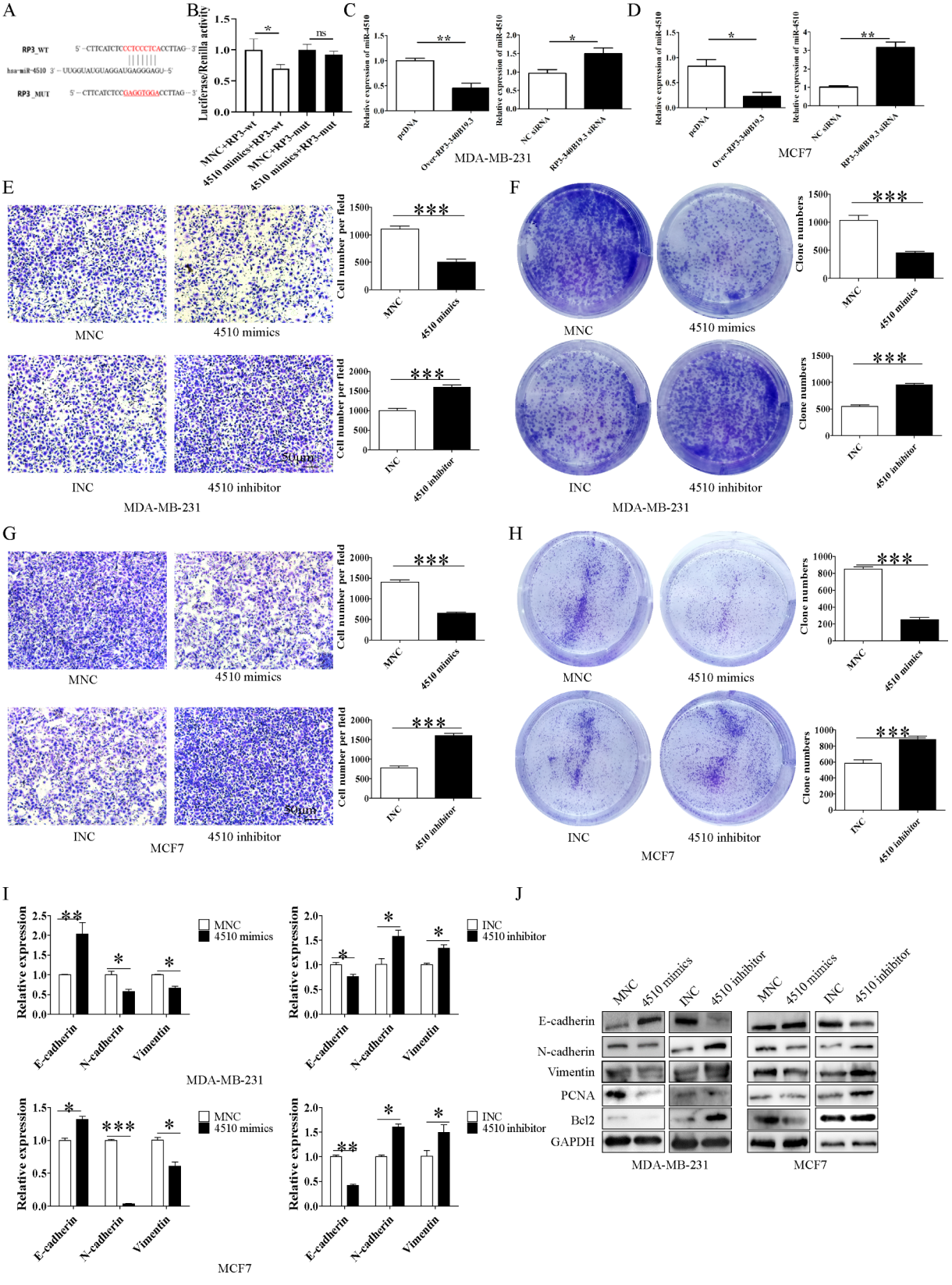

Fig. 4 (See legend on next page.)

(See figure on previous page.)

Fig. 4 RP3-340B19.3 targets and inhibits miR-4510. (**A**) The predicted binding sites in the seed region of RP3-340B19.3 and miR-4510. (**B**) The effect of miR-4510 on the stability of RP3-340B19.3 was determined by using a luciferase reporter gene assay. *$P < 0.05$. (**C**) and (**D**)The expression of miR-4510 in breast cancer cells transfected with pcDNA, RP3-340B19.3 overexpression plasmids, NC siRNA, and RP3-340B19.3 siRNA was examined by qRT-PCR. **$P < 0.01$, *$P < 0.05$. (**E**) and (**G**) The migratory ability of NC mimics, miR-4510-mimics, NC inhibitor and miR-4510 inhibitor transfected cells was evaluated by using transwell migration assay. ***$P < 0.001$. (F) and (H) Cell colony formation in NC mimics, miR-4510-mimics, NC inhibitor and miR-4510 inhibitor transfected cells. ***$P < 0.001$. (**I**) The expression of EMT related genes in NC mimics, miR-4510-mimics, NC inhibitor and miR-4510 inhibitor transfected cells was examined by qRT-PCR. ***$P < 0.001$, **$P < 0.01$, *$P < 0.05$. (**J**) The expression of EMT related proteins, PCNA and Bcl2 in NC mimics, miR-4510-mimics, NC inhibitor and miR-4510 inhibitor transfected cells was examined by western blot

Discussion

LncRNAs are crucial regulators of gene expression, and their dysregulated expression is intricately linked to the initiation and progression of tumours [21–23]. Our findings underscore the significant overexpression of RP3-340B19.3 within breast cancer cells exhibiting robust metastatic capabilities. Employing RNA fluorescence in situ hybridization technology, we observed that RP3-340B19.3 localized to both the nucleus and cytoplasm of breast epithelial cells MCF-10 A, as well as breast cancer cells MCF-7 and MDA MB-231. Moreover, the expression level of RP3-340B19.3 in these two breast cancer cell lines was notably elevated compared to normal breast epithelial cells MCF-10 A. This dysregulated expression of RP3-340B19.3 might exert a pivotal biological influence on the metastatic processes of breast cancer.

To elucidate the biological role of RP3-340B19.3, we conducted experiments involving breast cancer cells with varying metastatic capacities. Upon inducing high expression of RP3-340B19.3, cells with both high and low metastatic potential exhibited divergent levels of increased clonogenicity and migratory capabilities. Conversely, knockdown of RP3-340B19.3 led to diminished capacities in both cell lines. Similar to the functions of lncRNA-HIT [22], RP3-340B19.3 also influences cellular epithelial-mesenchymal transition (EMT). In a nude mouse subcutaneous tumour model, the RP3-340B19.3 knockdown group exhibited notably smaller tumour volumes and weights compared to the control group. Immunohistochemical analysis indicated a significant reduction in tumour tissue metastatic potential in the RP3-340B19.3 knockdown group. This reduction was attributed to a marked decrease in E-cadherin expression, accompanied by elevated N-cadherin and Vimentin levels. Additionally, decreased PCNA expression further indicated that reduced RP3-340B19.3 levels in vivo contributed to inhibiting breast cancer proliferation. In summary, our comprehensive approach, spanning cellular biology, protein levels, and animal experiments, revealed that RP3-340B19.3 fosters cell proliferation, hinders apoptosis, and triggers EMT, thus influencing breast cancer progression. These findings furnish fresh insights into the biological role of RP3-340B19.3 in breast cancer.

TME is composed of various cellular and non-cellular factors, all of which can influence the diagnosis, prognosis, and therapeutic efficacy of breast cancer [24]. BMMSCs are vital components in the tumour microenvironment. Their functions are widely restricted and regulated by the other components in TME, such as tumour cells [25]. Wu et al. found that lncRNA NEAT1 from MSC could confer gemcitabine resistance in pancreatic cancer via miR-491-5p/Snail/SOCS3 axis. We collected exosomes with high or low expression of RP3-340B19.3 from MDA-MB-231 cells and used them to treat target cells. BMMSCs and low metastatic breast cancer cells MCF7 treated with RP3-340B19.3 enriched exosomes showed increased proliferation and migration abilities, whereas exosomes with knocked-down RP3-340B19.3 had the opposite effect. These findings suggested that exosomes could transfer bioactive RP3-340B19.3 to breast cancer microenvironmental cells and promoted their proliferation and migration. This further indicated that exosomes derived from breast cancer cells promoted breast cancer progression by affecting breast cancer cells via transfer of RP3-340B19.3.

To delve into the molecular mechanisms underlying the biological functions of RP3-340B19.3, we initially examined the activation of relevant signaling pathways. Our investigation revealed that breast cancer cells overexpressing RP3-340B19.3 exhibited elevated levels of p65 phosphorylation, along with increased expression of genes from the Wnt family including Wnt2, Wnt3, Wnt5, and augmented levels of β-catenin. These findings strongly indicate that RP3-340B19.3 can activate both the Wnt/β-catenin and NF-κB signaling pathways, thereby promoting breast cancer proliferation and metastasis. Given the presence of RP3-340B19.3 in the cytoplasm of both breast epithelial and cancer cells, we hypothesize its role in breast cancer progression as a competing endogenous RNA (ceRNA). Through bioinformatics prediction and analysis, we identified a binding site for miR-4510 on RP3-340B19.3. Subsequent luciferase reporter gene experiments and functional studies confirmed that miR-4510 can indeed bind to RP3-340B19.3 and negatively regulate its expression. Moreover, miR-4510 was found to inhibit breast cancer cell proliferation and migration. The expression level of miR-4510 displayed a significant negative correlation with tumour diameter and pathological type, suggesting its potential role in breast cancer regulation. Further exploration of miR-4510's mechanism in promoting breast cancer proliferation and metastasis unveiled MORC4 as a direct target gene. Notably,

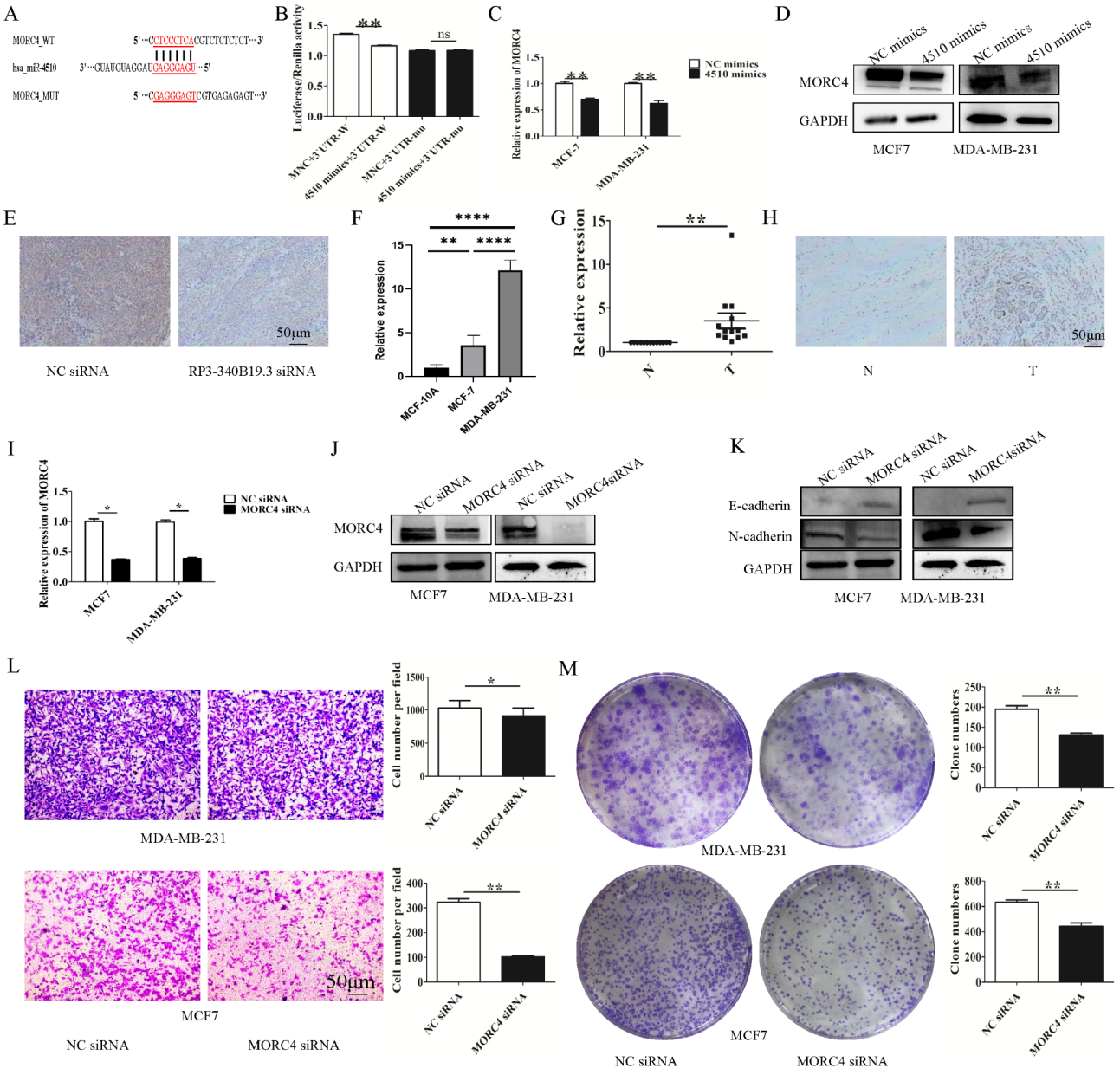

Fig. 5 miR-4510 targets and inhibits MORC4. (**A**) The predicted binding sites in the seed region of miR-4510 and the 3'UTR of MORC4 mRNA. (**B**) The effect of miR-4510 on the stability of MORC4 mRNA was determined by using a luciferase reporter gene assay. $^{**}P < 0.01$. (**C**) and (**D**) The expression of MORC4 in breast cancer cells transfected with MNC, and 4510 mimics was examined by qRT-PCR and western blot. $^{**}P < 0.01$. (**E**) The expression of MORC4 in mice transplanted with MDA-MB-231 cells pretreated with NC siRNA and RP3-340B19.3 siRNA was determined by immunohistochemistry. (**F**) The expression of MORC4 in MCF10A, MCF7 and MDA-MB-231 was examined by qRT-PCR. $^{**}P < 0.01$. (**G**) The mRNA levels of MORC4 in breast cancer tissues and adjacent normal tissues. $^{**}P < 0.01$. N, adjacent normal tissues; T, breast cancer tissues. (**H**) The protein levels of MORC4 in breast cancer tissues and adjacent normal tissues was determined by using immunohistochemistry. (**I**) and (**J**) The expression of MORC4 in breast cancer cells transfected with NC siRNA and MORC4 siRNA was examined by qRT-PCR and western blot. (**K**) The expression of EMT related proteins in NC siRNA, MORC4 siRNA transfected cells was examined by western blot. (**L**) The migratory ability of NC siRNA and MORC4 siRNA transfected cells was evaluated by transwell migration assay. $^{**}P < 0.01$, $^{*}P < 0.05$. (**M**) Cell colony formation in NC siRNA and MORC4 siRNA. $^{**}P < 0.01$

MORC4's involvement in cancer progression has been documented in other contexts. For instance, in colorectal cancer, MORC4 modulates the expression of PCGF1 and CDKN1A, while miR-193b-3p regulates MORC4 to promote apoptosis in breast cancer cells [26]. Consistent with these reports, our study indicated that MORC4 expression in breast cancer tissue was lower than that in normal breast tissue, confirming its negative correlation with miR-4510. Thus, our findings suggest that RP3-340B19.3 facilitates MORC4 expression by sequestering

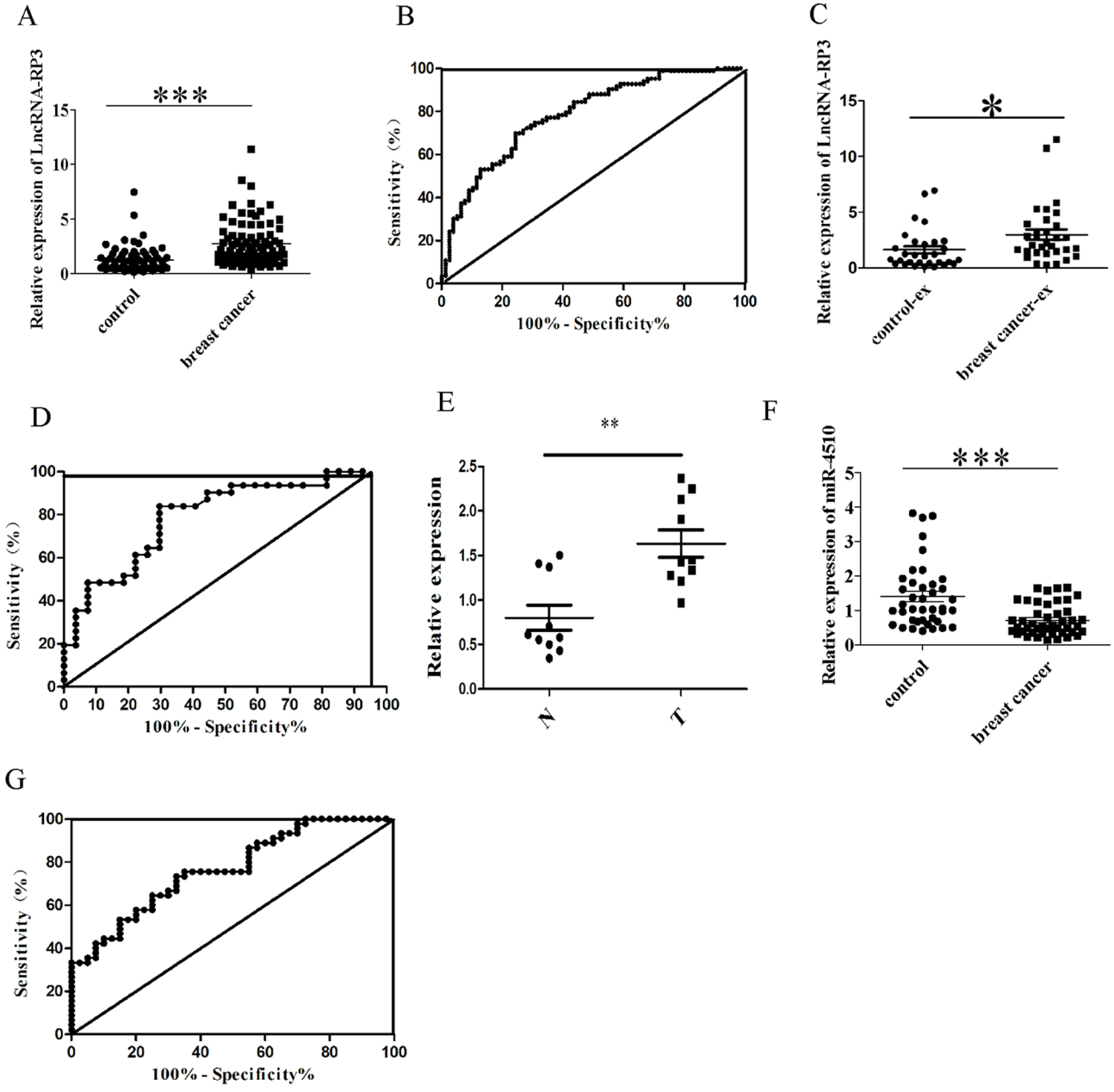

Fig. 6 Clinical detection analysis of RP3-340B19.3 in serum and its exosomes. (**A**) The expression of RP3-340B19.3 in the serum of 66 patients with breast cancer and that of 66 healthy volunteers. ***$P < 0.001$. (**B**) ROC curves for the diagnostic values of RP3-340B19.3 in breast cancer. (**C**) The expression of exosomal RP3-340B19.3 in the serum of 27 patients with breast cancer and that of 27 healthy volunteers. ***$P < 0.001$. (**D**) ROC curves for the diagnostic values of serum CA153 and exosomal RP3-340B19.3 in breast cancer. (**E**) The expression of RP3-340B19.3 in 10 breast cancer tissues and 10 adjacent normal tissues was determined by quantitative RT-PCR. *$P < 0.05$. N, adjacent normal tissues; T, breast cancer tissues. (**F**) The expression of miR-4510 in the serum of 35 patients with breast cancer and that of 35 healthy volunteers. ***$P < 0.001$. (**G**) ROC curves for the diagnostic values of miR-4510 in breast cancer

miR-4510, thereby fostering breast cancer cell proliferation and migration.

LncRNAs are known to be dysregulation in various tumour types and serve as valuable biomarkers for tumour diagnosis, efficacy monitoring, and metastasis assessment [27–29]. Specifically, in the context of triple-negative breast cancer (TNBC), certain lncRNAs, including RP11-434D9.1, LINC00052, BC016831, and IGKV, exhibit low expression levels. Remarkably, the expression levels of these four lncRNAs enable effective differentiation between TNBC and non-TNBC cases [30]. Furthermore, the significance of HOTTIP extends to predicting poor prognosis associated in breast cancer. Elevated expression of HOTTIP correlates with unfavorable outcomes, as evidenced by lower overall survival rates

Table 1 Correlation between RP3-340B19.3 in breast cancer tissues and clinicopathological parameters

Clinicopathological information	*n*	Relative expression of RP3	*P*
Tumor diameter			
<=2 cm	29	1.817(1.440, 2.195)	0.0281
> 2 cm	37	2.685(2.138, 3.231)	
Age			
< 50	15	1.815(1.350, 2.280)	0.2449
≥ 50	51	2.447(2.008, 2.887)	
Pathological type			
Invasive ductal carcinoma	54	2.505(2.091, 2.919)	0.0123
Ductal carcinoma in situ and others	12	1.399(1.097, 1.700)	
Lymph node metastasis			
0	38	2.138(1.656, 2.620)	0.1091
>=1	28	2.528(1.977, 3.080)	
TNM staging			
0 + I	22	1.437(1.109, 1.764)	0.1353
II	27	2.768(2.046, 3.491)	
III	17	2.203(1.686, 2.719)	
HER-2			
-	39	2.443(1.924, 2.962)	0.4813
+	27	2.103(1.628, 2.577)	

Table 2 Correlation between exo-RP3-340B19.3 in breast cancer tissues and clinicopathological parameters

Clinicopathological information	*n*	Relative expression of exo-RP3	*P*
Tumor diameter			
<=2 cm	11	1.842(1.339, 2.345)	0.0198
> 2 cm	16	4.141(2.470, 5.812)	
Age			
≤ 50	9	2.254(1.099, 3.410)	0.1763
>50	18	3.679(2.166, 5.192)	
Pathological type			
Invasive ductal carcinoma	22	3.330(2.062, 4.598)	0.6065
Ductal carcinoma in situ and others	5	2.648(0.331, 4.965)	
Lymph node metastasis			
0	14	2.526(1.536, 3.517)	0.1279
>=1	13	3.934(1.900, 5.968)	
TNM staging			
0 + I	5	2.702(0.454, 4.950)	0.5840
II	17	3.087(1.725, 4.449)	
III	5	4.104(0, 8.778)	
HER-2			
-	10	3.520(1.471, 5.569)	0.4143
+	17	3.018(1.657, 4.380)	

and reduced disease-free survival rates among breast cancer patients [31].

In recent years, research has revealed the advantages of utilizing exosomes in tumour diagnosis. Exosomes proffer distinctive advantages, notably their facile preservation, capacity to delineate the intricate trajectory of tumour development, and their rich reservoir of bioactive molecules, thereby endowing them with pronounced clinical relevance [32, 33]. Exosomes, characterized by a diameter of approximately 40–100 nm, manifest as circular or elliptical membranous vesicles [34]. These vesicles can be secreted by various cells and contain proteins and nucleic acid molecules associated with their parent cells. Bioactive molecules derived from exosomes, including proteins and non-coding RNAs, have demonstrated their efficacy as sensitive and specific diagnostic biomarkers for tumours [35–37]. Notably, the expression level of CRNDE-h in extracellular vesicles within the serum of colon cancer patients exhibits a significant correlation with regional lymph node metastasis and distant metastasis. This particular expression serves as a diagnostic and prognostic marker for colon cancer [38].

Table 3 Correlation between miR-4510 in breast cancer tissues and clinicopathological parameters

Clinicopathological information	*n*	Relative expression of miR-4510	*P*
Tumor diameter			
<=2 cm	16	0.878(0.617, 1.139)	0.0479
> 2 cm	19	0.527(0.418, 0.636)	
Age			
≤ 50	10	0.800(0.506, 1.093)	0.2253
>50	25	0.643(0.476, 0.809)	
Pathological type			
Invasive ductal carcinoma	26	0.595(0.451, 0.739)	0.0115
Ductal carcinoma in situ and others	9	0.955(0.615, 1.294)	
Lymph node metastasis			
0	23	0.753(0.562, 0.944)	0.1955
>=1	12	0.561(0.369, 0.753)	
TNM staging			
0(DICS)	7	0.772(0.377, 1.168)	0.6730
I	8	0.798(0.369, 1.226)	
II	14	0.580(0.375, 0.784)	
III	6	0.693(0.295, 1.090)	
HER-2			
-	21	0.639(0.453, 0.825)	0.3088
+	14	0.760(0.526, 0.994)	

The expression level of RP3-340B19.3 was markedly elevated in breast cancer tissues, breast cancer patients, serum, and serum-derived exosomes compared to adjacent tissues and healthy individuals. This notable upregulation indicates its prospective significance as a novel molecular marker for breast cancer diagnosis, offering a non-invasive diagnostic avenue. Evaluation of serum RP3-340B19.3 levels, in conjunction with clinical and pathological data, unveiled a significant correlation between its expression and both tumour diameter and pathological type. Particularly, a positive correlation was discerned between serum RP3-340B19.3 expression and tumour diameter. Furthermore, its expression was

found to be higher in invasive ductal carcinoma compared to ductal carcinoma in situ and other pathological types. Similarly, analysis of serum exosome-bound RP3-340B19.3 in conjunction with clinical-pathological data demonstrated a substantial correlation with tumour diameter, while associations with other pathological features were not observed. Notably, patients with larger tumour diameters manifested elevated levels of Exo-RP3-340B19.3. Importantly, breast cancer patients displaying elevated expression levels of RP3-340B19.3 in both serum and serum-derived exosomes exhibited a poorer prognosis. This underscored the potential prognostic value of RP3-340B19.3 as a predictive marker in breast cancer outcomes.

Conclusion

In conclusion, this study has identified the role of RP3-340B19.3 both in vivo and in vitro breast cancer contexts. It delved into the associated molecular mechanisms, thereby expanding our understanding of the novel functions and regulatory modes of the lncRNA RP3-340B19.3 in breast cancer proliferation and metastasis. The expression of RP3-340B19.3 was found to be up-regulated in breast cancer cells, tumour tissues, serum from breast cancer patients, as well as in their exosomes. This highlights its potential as a promising candidate for new diagnostic and therapeutic markers for breast cancer.

Supplementary Information

The online version contains supplementary material available at https://doi.org/10.1186/s12935-024-03490-3.

Supplementary Material 1

Supplementary Material 2

Supplementary Material 3

Supplementary Material 4

Author contributions

B.W. and JH.M performed and analyzed the experiments and wrote the manuscript. LX.W and YX.Z helped to perform the experiments. H.Y and BY.W designed and supervised the study. B.W and JH.M contributed equally to this work.

Funding information

This study was supported by the National Natural Science Foundation of China (grant no.81702078); the Natural Science Foundation of Jiangsu Province (grant no.BK20170356); Suzhou Science, Education and Health Youth Science and Technology Project (grant no.KJXW2020019);Gusu Talent Program (GSWS2023041); Support for the project of nuclear technology medical application supported by discipline construction (grant no.XKTJ-HRC2021001); Science and Technology Program of Suzhou (grant no.SKY2021045, SKJY2021097); Maternal and Child Health Association Project of Jiangsu province (grant no.FYX202123); The Key Research and Development Project of Zhenjiang (grant no. SH2022044); "National Tutor System"Training Program for Health Youth Key Talents in Suzhou(Qngg2023008).

Data availability

No datasets were generated or analysed during the current study.

Declarations

Ethics approval and consent to participate

The studies involving human participants were reviewed and approved by Ethics Committee of the Second Affiliated Hospital of Soochow University. The animal study was reviewed and approved by Experimental Animal Ethics Committee of Soochow University.

Consent for publication

Not applicable.

Competing interests

The authors declare no competing interests.

Author details

[1]Department of Oncology, The Second Affiliated Hospital of Soochow University, Suzhou, China
[2]Department of Central Laboratory, The Affiliated Hospital of Jiangsu University, Zhenjiang, China
[3]Department of Clinical Laboratory, The Second Affiliated Hospital of Soochow University, Suzhou, China

Received: 20 November 2023 / Accepted: 24 August 2024
Published online: 10 September 2024

References

1. Siegel RL, Miller KD, Fuchs HE, Jemal A. Cancer statistics, 2022. CA Cancer J Clin. 2022;72(1):7–33.
2. Jokar N, Velikyan I, Ahmadzadehfar H, Rekabpour SJ, Jafari E, Ting HH, et al. Theranostic Approach in breast Cancer: a treasured tailor for future oncology. Clin Nucl Med. 2021;46(8):e410–20.
3. Hutchinson L. Breast cancer: challenges, controversies, breakthroughs. Nat Rev Clin Oncol. 2010;7(12):669–70.
4. Ghafouri-Fard SM, Taheri. Long non-coding RNA signature in gastric cancer. Exp Mol Pathol. 2020;113:104365.
5. Chi Y, Wang JP, Yu WD, Yang JC. Long non-coding RNA in the pathogenesis of cancers. Cells. 2019;8(9):1015.
6. Kristensen LS, Andersen MS, Stagsted LVW, Ebbesen KK, Hansen TB, Kjems J. The biogenesis, biology and characterization of circular RNAs. Nat Rev Genet. 2019;20(11):675–91.
7. Zhang Y, Liang W, Zhang P, Chen JY, Qian H, Zhang X, Xu WR. Circular RNAs: emerging cancer biomarkers and targets. J Exp Clin Cancer Res. 2017;36(1):152.
8. Chen XY, Mao R, SuWM, Yang X, Geng QQ, Guo CF, et al. Circular RNA circHIPK3 modulates autophagy via MIR124-3p-STAT3-PRKAA/AMPKalpha signaling in STK11 mutant lung cancer. Autophagy. 2020;16(4):659–71.
9. Du WW, Yang WN, Liu E, Yang ZG, Dhaliwal P, Yang BB. Foxo3 circular RNA retards cell cycle progression via forming ternary complexes with p21 and CDK2. Nucleic Acids Res. 2016;44(6):2846–58.
10. Ghetti M, Vannini I, Storlazzi CT, Martinelli G, Simonetti G. Linear and circular PVT1 in hematological malignancies and immune response: two faces of the same coin. Mol Cancer. 2020;19(1):69.
11. Zhang ML, Zhao K, Xu XP, Yang YB, Yan S, Wei P, et al. A peptide encoded by circular form of LINC-PINT suppresses oncogenic transcriptional elongation in glioblastoma. Nat Commun. 2018;9(1):4475.
12. Zhang YX, Dong XT, Guo XY, Li CS, Fan YP, Liu PJ, et al. LncRNA-BC069792 suppresses tumor progression by targeting KCNQ4 in breast cancer. Mol Cancer. 2023;22(1):41.
13. Zhao WY, Geng DH, LiSQ, Chen ZF, Sun M. LncRNA HOTAIR influences cell growth, migration, invasion, and apoptosis via the miR-20a-5p/HMGA2 axis in breast cancer. Cancer Med. 2018;7(3):842–55.
14. Yue X, Wu WY, Dong M, Guo M. LncRNA MALAT1 promotes breast cancer progression and doxorubicin resistance via regulating miR-570-3p. Biomed J. 2021;44(6 Suppl 2):S296–304.
15. Zhang X, Yuan X, Shi H, Wu LJ, Qian H, Xu WR. Exosomes in cancer: small particle, big player. J Hematol Oncol. 2015;8:83.
16. Thery C, Zitvogel L, Amigorena S. Exosomes: composition, biogenesis and function. Nat Rev Immunol. 2002;2(8):569–79.
17. Yu D, Li YX, Wang MY, Gu JM, Xu WR, Cai H, et al. Exosomes as a new frontier of cancer liquid biopsy. Mol Cancer. 2022;21(1):56.

18. Ni C, Fang QQ, Chen WZ, Jiang JX, Jiang Z, Ye J, et al. Breast cancer-derived exosomes transmit lncRNA SNHG16 to induce CD73 + gammadelta1 Treg cells. Signal Transduct Target Ther. 2020;5(1):41.
19. Liu C, Lu C, Yixi L, Hong JX, Dong F, Ruan SN, et al. Exosomal Linc00969 induces trastuzumab resistance in breast cancer by increasing HER-2 protein expression and mRNA stability by binding to HUR. Breast Cancer Res. 2023;25(1):124.
20. Yang H, Wang B, Xu LJ, He CY, Wen HY, Yan J, et al. Toll-like receptor 4 prompts human breast cancer cells invasiveness via lipopolysaccharide stimulation and is overexpressed in patients with lymph node metastasis. PLoS ONE. 2014;9(10):e109980.
21. Zhu XM, Zhang HZ, Xu J. Long noncoding RNA SNHG20 regulates cell migration, invasion, and proliferation via the microRNA-19b-3p/RAB14 axis in oral squamous cell carcinoma. Bioengineered. 2021;12(1):3993–4003.
22. Richards EJ, Zhang G, Li ZP, Permuth-Wey J, Challa S, Li YJ, et al. Long non-coding RNAs (LncRNA) regulated by transforming growth factor (TGF) beta: LncRNA-hit-mediated TGFbeta-induced epithelial to mesenchymal transition in mammary epithelia. J Biol Chem. 2015;290(11):6857–67.
23. Ma JY, Liu SH, Chen J, Liu Q. Metabolism-related long non-coding RNAs (lncRNAs) as potential biomarkers for predicting risk of recurrence in breast cancer patients. Bioengineered. 2021;12(1):3726–36.
24. Deepak KGK, Vempati R, Nagaraju GP, Dasari VR, Rao SN. Tumor microenvironment: challenges and opportunities in targeting metastasis of triple negative breast cancer. Pharmacol Res. 2020;153:104683.
25. ZhangT, Lee YW, Rui YF, Cheng TY, Jiang XH, Li G. Bone marrow-derived mesenchymal stem cells promote growth and angiogenesis of breast and prostate tumors. Stem Cell Res Ther. 2013;4(3):70.
26. Yang Z, Zhuang QL, Hu GF, Geng SK. MORC4 is a novel breast cancer oncogene regulated by miR-193b-3p. J Cell Biochem. 2019;120(3):4634–43.
27. Xing C, Sun SG, Yue ZQ, Bai F. Role of lncRNA LUCAT1 in cancer. Biomed Pharmacother. 2021;134:111158.
28. Zhi H, Yang DY, Fan XL, Zhang MW, Li Y, Gu XB, et al. The roles and mechanisms of lncRNAs in Liver Fibrosis. Int J Mol Sci. 2020;21(4):1482.
29. Poulet C, Njock M, Moermans C, Louis E, Louis R, Malaise M, et al. Exosomal Long non-coding RNAs in Lung diseases. Int J Mol Sci. 2020;21(10):3580.
30. Lv M, Xu PF, Wu Y, Huang L, Li WQ, Lv SS, et al. LncRNAs as new biomarkers to differentiate triple negative breast cancer from non-triple negative breast cancer. Oncotarget. 2016;7(11):13047–59.
31. Yang YL, Qian JX, Xiang YQ, Chen YZ, Qu JM. The prognostic value of long noncoding RNA HOTTIP on clinical outcomes in breast cancer. Oncotarget. 2017;8(4):6833–44.
32. Zhang Y, Bi JY, Huang JY, Tang YN, Du SY, Li PY, Exosome. A review of its classification, isolation techniques, Storage, Diagnostic and targeted therapy applications. Int J Nanomed. 2020;15:6917–34.
33. Yang DB, Zhang WH, Zhang HY, Zhang FQ, Chen LM, Ma LX, et al. Progress, opportunity, and perspective on exosome isolation - efforts for efficient exosome-based theranostics. Theranostics. 2020;10(8):3684–707.
34. Boorn JGVD, Dassler J, Coch C, Schlee M, Hartmann G. Exosomes as nucleic acid nanocarriers. Adv Drug Deliv Rev. 2013;65(3):331–5.
35. Li Y, Zheng QP, Bao CY, Li SY, Guo WJ, Zhao J, et al. Circular RNA is enriched and stable in exosomes: a promising biomarker for cancer diagnosis. Cell Res. 2015;25(8):981–4.
36. Zhou WY, Fong M, Min YF, Somol G, Liu L, Palomares MR, et al. Cancer-secreted miR-105 destroys vascular endothelial barriers to promote metastasis. Cancer Cell. 2014;25(4):501–15.
37. Soldevilla B, Rodriguez M, Millan CS, Garcia V, Perianez RF, Calderon BG, et al. Tumor-derived exosomes are enriched in DeltaNp73, which promotes oncogenic potential in acceptor cells and correlates with patient survival. Hum Mol Genet. 2014;23(2):467–78.
38. Liu T, Zhang X, Gao SY, Jing FM, Yang YM, Du LT, et al. Exosomal long noncoding RNA CRNDE-h as a novel serum-based biomarker for diagnosis and prognosis of colorectal cancer. Oncotarget. 2016;7(51):85551–63.

Publisher's note